Study of steel mass spring system with varying speeds in a tunnel

Aamir Rashid Chowdhary[1,2,*] and Nasim Akhtar[2]

[1]Academy of Scientific and Innovative Research, Ghaziabad 201 002, India
[2]CSIR-Central Road Research Institute, New Delhi 110 025, India

A steel mass spring system (MSS) has been designed using the Zimmermann method. The impact of speed on the curve radius, cant, stiffness, static and dynamic deflection of the MSS is observed and the natural frequency of the system is calculated. It has been observed that the speed of the train affects the stiffness of MSS and therefore the insertion loss. As the speed of the train increases, the characteristic length of the floating slab track decreases due to which the spacing between MSS also changes. Hence this design of MSS will be effective.

Keywords: Floating slab track, mass spring system, natural frequency, tunnel, vibration.

SINCE railway transportation is energy-efficient and generates fewer emissions, it has become increasingly common as a result of global warming. Railway technology has advanced, resulting in increased mobility and convenience as well as an appealing, modern and environment-friendly mode of transportation. The extension of the railway network, on the other hand, has raised environmental concerns. Near railway and transit routes, vibration and noise have a significant effect. In urban areas, the metro lines mostly run under existing developing units. As such, there are many complaints from residents regarding the noise and vibration generated by the metro operation. These issues are due to resistance and reverberations over the wheel–rail contact. This vibration is adequately transmitted through the ground to the neighbouring buildings along the line, affecting the residents. The track vibration is caused by trains running on the track, due to roughness of the wheels, rail corrugation, grinding of wheels and rails, discontinuous rail and unsmooth track-supporting structure. This causes tracking vibrations, which travel in a variety of ways, including the track system, tunnel structure, geotechnical condition, residential structure foundation and adjacent buildings. Any vibration above 200 Hz is not considered harmful, but it is subjected to a low frequency[1]. The most disturbing frequency range from the metro ranges from 45 to 50 Hz. The impact of vibrations of high amplitude for a short duration on humans can lead to injuries to the muscles or internal organs (<25 Hz frequency). Vibrations can also lead to the malfunctioning of sensitive equipment[2,3]. Therefore, measures to control environmental vibrations due to railway transportation should be both scientific and practical[4–7]. Vibration control can be attained by isolating the source[6], interrupting the vibration path[8] and/or isolating the receiver, i.e. buildings[9]. There are many vibration control products available worldwide. These include the Vanguard[10], Cologne Egg[11], Ladder track[12], magnetorheological fluids[13] and floating slab track (FST)[14]. FST is the best method to control vibrations in underground railway systems[15–17], which can be supported by rubber bearings, glass fibre, polyurethane (PU) or steel springs[18]. Normally, two types of mass spring system (MSS) are used in the floating chamber (Table 1). (a) Discrete MSS, i.e. steel MSS and rubber/PU MSS. (b) Full-surface MSS, i.e. PU/rubber MSS and rock wool MSS (density ≥ 350 kg/m^3)

FST provides an effective way to reduce the transmission of vibrations from railway traffic to the ground[19–21]. The vibration problems of an FST system have been extensively studied on the basis of theoretical methods[22–24] and experimental methods[25,26]. The calculation of vibrations generated by moving trains on MSS in underground railway tunnels requires a model that takes into account the dynamics and interaction between the train, tracks, tunnel and floor[27]. In addition to theoretical analysis, some laboratory and field tests have also been reported in the literature. The impact of stiffness and spacing of steel springs with low-frequency vibration tests was studied in Beijing Jiao Tong University, China[28]. The ability to reduce vibrations from the steel-spring FST of Beijing metro line 5 in China was tested[29]. On the other hand, energy transfer of the FST system in Singapore was analysed using an analytical method[30].

From the above, it can be seen that many theoretical and experimental research efforts have been dedicated to the dynamic properties of MSS and its impact on ground-borne vibration. However, few studies have been carried out on the influence of speed and curve radius, which are key technical parameters for MSS design in a tunnel. In FST, there are two stages of concrete in the tunnel. In the first stage, the height varies between 200 mm and 350 mm normally, while in the second stage it varies between 225 mm and 600 mm and above. MSS is installed between

*For correspondence. (e-mail: aamirrashid606@gmail.com)

Table 1. Different types of mass spring system (MSS)[36,37]

MSS	Steel MSS	Polyurethane (PUR)-discrete MSS	PUR-full-surface MSS
Natural frequency (Hz)	7–8	12–14	20
Attenuation start (Hz)	10–11	20	28.28
Global value killing (VdB)	26–28	15–17	9.6

the first and second stages of concrete. The gap between these two stages of concrete may vary between 20 mm and 60 mm depending on the availability of space inside the tunnel. The second stage of concrete plays an important role in controlling vibrations. As the depth of concrete increases, the natural frequency of MSS decreases accordingly, and thus the attenuation rate increases. In the case of a 5.8 m diameter tunnel, there are two types of electrical power supply to trains in India. One is overhead equipment (OHE) and the other is the third rail. In the case of OHE, on top of the tunnel system 1 m space should be kept and due to the height of MSS, it requires critical design. Whereas in the case of the third rail, the electrical power supply is on the ground and hence due to the availability of space, depth of concrete and space between the first and second stages of concrete can be controlled in the design. The third rail system has been adopted in Kolkata Metro Rail Corporation, and Ahmedabad Metro Rail Corporation, while the OHE system is used in the Pune Metro Rail Corporation, Nagpur Metro Rail Corporation, Mumbai Metro Rail Corporation, Chennai Metro Rail Corporation and Delhi Metro Rail Corporation. Where there is OHE, an increase of height in the second stage of concrete inside a tunnel is a difficult task. As a result, designers have a challenging problem in creating the gap between the first and second stages of concrete. The maximum value of the cant on horizontal curves should also be 1/10th to 1/12th of the gauge, which should be less than 140 mm (ref. 31). The maximum space for MSS can be 40 mm if the first stage of concrete is less than 250 mm. However, if the first stage concrete is 300 mm, then it becomes difficult to design the steel MSS due to limited space. This problem can be solved by providing discrete PU pads MSS or full surface PU MSS with a 20–30 mm gap. Full surface PU MSS has been installed in almost all metros in India. However, in terms of vibration control, they are not much effective. Due to this, steel MSS, discrete PU MSS, and Vanguard system are proposed to be used in other upcoming metros. The metros in India are designed for a speed of 90 kmph, while the operating speed is less than 70 kmph because the station to station distance is around 1 km. It has been observed that less vibrations are generated in the straight portion while on the curved portion, vibration increases drastically (Delhi metro). Normally, in the straight portion operating speed varies between 60 and 70 kmph, while on the curved portion (radius <450 m), it is around 50 kmph or less. In this study, we have taken a typical 5.8 m diameter tunnel and designed steel MSS with different varying conditions like speed, radius and cant. Different types of MSS specifications according to DIN EN 13906-1: 2013–11 have been used for fatigue tests for the design of MSS[32]. This study provides results for steel MSS based on different parameters like FST material parameters[33], rolling stock parameters[34], track parameters and elastic support parameters[32].

Evaluation of steel MSS using Zimmermann method

We have used the Zimmermann method for static and dynamic analysis for MSS design, calculation of vertical natural frequency, stiffness of MSS, fatigue verification, and calculation of insertion loss based on vertical natural frequency and damping ratio (spectral analysis in the third-octave band).

Spring unit used in the design

There are two types of spring in a housing – external and internal. The diameter of the external spring is 44 mm and the total number of turns is 3, while for the internal spring the diameter is 20 mm and the total number of turns is 5.6. Modulus of elasticity, $E = 206{,}000$ N/mm^2 and shear modulus, $G = 78{,}500$ N/mm^2. The height of the block is less than 185 mm.

The vertical spring rate (k_v) and horizontal spring rate (k_H) are expressed as follows

$$k_v = G\frac{d^4}{8nD^3}, \tag{1}$$

$$k_{\text{Hstatic + dyn}} = \eta_{\text{static + dyn}} \cdot k_v, \tag{2}$$

where G is shear modulus, d the diameter of the spring, n the number of turns, D the spring housing diameter and η is the ratio of horizontal to vertical spring rate.

To calculate the fatigue strength of MSS, the stresses in the external and internal springs on the outside and inside track are calculated.

Maximum vertical spring load

$$V_{\text{static + dyn VER}} = Gd^4 d_{\text{static + dyn MAX}} / 8nD^3. \tag{3}$$

Maximum horizontal spring load

$$H_{\text{static + dyn VER}} = k_{\text{Hstatic + dyn}} d_{\text{dstatic+dyn HOR,}} \quad (4)$$

where $d_{\text{static + dyn VER}}$ is vertical deflection and $d_{\text{static + dyn HOR}}$ is the horizontal deflection.

Rail Type-UIC 60

The UIC 60 rail has been used having a modulus of elasticity of rails, $E_{\text{RAIL}} = 2.10\text{E} + 08$ kN/m^2, rail height, $h_{\text{RAIL}} = 172$ mm, the second moment of area of rails, $I_{\text{RAIL}} = 3055$ cm^4, area of the cross-section of the rails. $A_{\text{RAIL}} = 76.87$ cm^2, mass per linear metre of rail, $\mu_{\text{RAIL}} = 60.34$ kg/m, centre of gravity, $z_{\text{CG}} = 80.9$ mm and mass per linear metre of the fasteners $\mu_{\text{FAST}} = 92.3$ kg/m (ref. 35).

FST cross-section properties

Figure 1 shows the cross-section of the tunnel with diameter 5.8 m, UIC 60 rail, stage II and stage I concrete as well as steel MSS. Figure 2 shows the FST cross-section.

For designing steel MSS, the following equations have been used

$$\text{Cant, } s = \text{bit}.v^2/gR, \quad (5)$$

where bit is the gauge length, v the speed of the train, g the acceleration due to gravity and R is the curve radius.

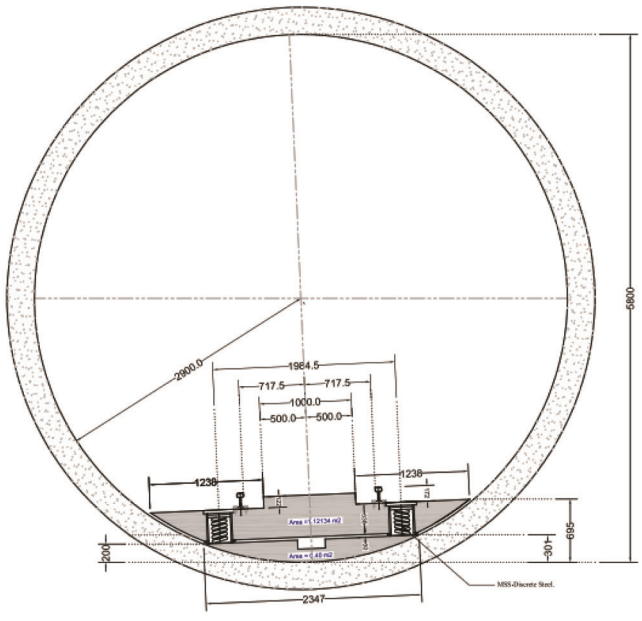

Figure 1. Typical cross-section of steel mass spring system (MSS) inside a tunnel of diameter 5.8 m.

The cross-sectional area (CoG), and linear mass of FST are calculated for determining the vertical natural frequency of MSS as

Cross-sectional area of FST

$$A_{\text{conc transv}} = bh + 2(h_1 b_1) + h_1 b_2 + 2(hb_3)/2. \quad (6)$$

CoG of the track bed

$$\text{CoG}_{\text{FST}} = (A_{\text{con transv}}\delta_{\text{conc}}\text{CoG}_{\text{slab}} + 2A_{\text{rail}}\delta_{\text{steal}}(h + h_1 + Z_{\text{CG}}))/ (A\delta_{\text{conc}} + 2A_1\delta_{\text{conc}} + 2A_{\text{rail}}\delta_{\text{steal}}). \quad (7)$$

Linear mass of FST

$$\mu_{\text{FST}} = A_{\text{conc transv}}\delta_{\text{conc}} + 2\mu_{\text{Rail}} + \mu_{\text{FAST}}. \quad (8)$$

Using eqs (6)–(8), the second moment of area of FST is calculated as follows

$$\begin{aligned} Iy_{\text{FST}} = {} & [bh^3/12 + bh(\text{CoG}_{\text{FST}} - h/2)^2 \\ & + [2(b_1h_1^3/12 + b_1h_1(\text{CoG}_{\text{FST}} - h_1/2)^2)] \\ & + [(b_2h_1^3/12 + b_2h_1(\text{CoG}_{\text{FST}} - h_1/2)^2)] \\ & + [2(b_3h^3/36 + b_3h(\text{CoG}_{\text{FST}} - h/2)^2)] \\ & + [2(I_{\text{RAIL}} + A_{\text{RAIL}}(\text{CoG}_{\text{FST}} - (h + z_{\text{CG}})^2)]]. \end{aligned} \quad (9)$$

Also, the modulus of rigidity of FST is calculated as

$$EI_{\text{FST}} = E_{\text{conc}}(I_{\text{CoG}} + I_{\text{l}_{\text{CoG}}}) + E_{\text{RAIL}} I_{\text{RAIL}_{\text{CoG}}}. \quad (10)$$

FST stiffness

The stiffness of FST depends on the spring rate and longitudinal spacing outside and inside of the curve. It has been calculated using the following equations.

Vertical stiffness per metre length of outside FST

$$k_{v_{\text{FST}_{\text{out}}}} = k_v/\text{spac}_{\text{long}_{\text{out}}}. \quad (11)$$

Vertical stiffness per metre length of inside FST

$$k_{\text{v}_{\text{FST}_{\text{in}}}} = k_v/\text{spac}_{\text{long}_{\text{in}}}. \quad (12)$$

Horizontal stiffness per metre length of outside FST

$$k_{\text{H}_{\text{FST}_{\text{out}}}} = k_{\text{H}}/\text{spac}_{\text{long}_{\text{out}}}. \quad (13)$$

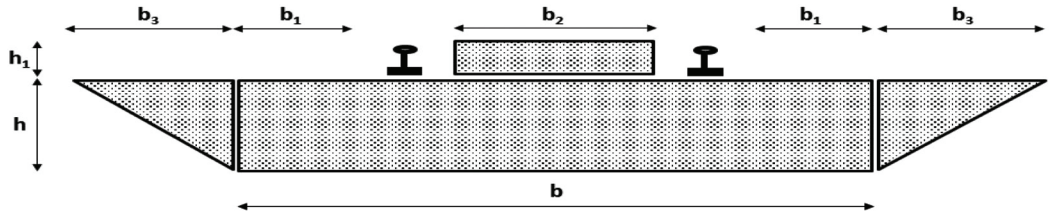

Figure 2. Floating slab track cross-section.

Horizontal stiffness per metre length of inside FST

$$k_{\mathrm{H}_{\mathrm{FST}_{\mathrm{in}}}} = k_{\mathrm{H}}/\mathrm{spac}_{\mathrm{long}_{\mathrm{in}}}. \quad (14)$$

Using eqs (11)–(14), the vertical and horizontal stiffness values per metre length of FST are calculated as follows

Vertical stiffness per metre length of FST

$$k_{v_{\mathrm{FST}}} = k_v/\mathrm{spac}_{\mathrm{long}_{\mathrm{out}}} + k_v/\mathrm{spac}_{\mathrm{long}_{\mathrm{in}}}. \quad (15)$$

Horizontal stiffness per metre length of FST

$$k_{\mathrm{H}_{\mathrm{FST}}} = k_{\mathrm{H}}/\mathrm{spac}_{\mathrm{long}_{\mathrm{out}}} + k_{\mathrm{H}}/\mathrm{spac}_{\mathrm{long}_{\mathrm{in}}}, \quad (16)$$

where $\mathrm{spac}_{\mathrm{long}_{\mathrm{out}}}$ is the longitudinal spacing outside the curve, $\mathrm{spac}_{\mathrm{long}_{\mathrm{in}}}$ the longitudinal spacing inside the curve, k_v the vertical spring rate and k_H the horizontal spring rate.

Load combinations to calculate natural frequency and fatigue verification

The results of static load and centrifugal force caused by train operation are calculated as follows

Static load (FST weight), $F_{\mathrm{FST}} = \mu \cdot g$. (17)

Centrifugal force $F_{\mathrm{centr}} = (F_{\mathrm{vert\ axle}}/g)(v^2/R)$. (18)

Resultant load to calculate natural frequency

To calculate natural frequency, the resultant vertical load outside and inside the wheel is calculated.

Resultant vertical load outside the wheel for v = 30, 50, 70, 80 and 90 kmph is

$$F_{\mathrm{res}_{\mathrm{V}_{\mathrm{out}}}} = (F_{\mathrm{vert}_{\mathrm{V}}} + F_{\mathrm{centr}_{\mathrm{V}}})/$$

$$2 + [(h + h_{\mathrm{l}} + h_{\mathrm{RAIL}} + \mathrm{cog})/\mathrm{spac}_{\mathrm{TRANSV}}](F_{\mathrm{centr}_{\mathrm{H}}} - F_{\mathrm{vert}_{\mathrm{V}}}), \quad (19)$$

where $\mathrm{spac}_{\mathrm{TRANSV}}$ is the transverse spacing between spring units = 2 m.

Resultant vertical load inside the wheel for v = 30, 50, 70, 80 and 90 kmph is

$$F_{\mathrm{res}_{\mathrm{V}_{\mathrm{in}}}} = (F_{\mathrm{vert}_{\mathrm{V}}} + F_{\mathrm{centr}_{\mathrm{V}}})/$$

$$2 - [(h + h_{\mathrm{l}} + h_{\mathrm{RAIL}} + \mathrm{cog})/\mathrm{spac}_{\mathrm{TRANSV}}](F_{\mathrm{centr}_{\mathrm{H}}} - F_{\mathrm{vert}_{\mathrm{V}}}). \quad (20)$$

Using eqs (10) and (15), the characteristic length of FST is calculated as

$$L_{\mathrm{charact}} = (4EI_{\mathrm{FST}}/k_{v_{\mathrm{FST}}})^{1/4}, \quad (21)$$

where $k_{v_{\mathrm{FST}}}$ is the stiffness (spring rate) per metre = modulus of subgrade × width of FST.

FST dynamic vertical deflections

The speed of the train directly affects the dynamic vertical deflections both outside and inside the wheel. Using eqs (22) and (23), the maximum dynamic deflection for determining the fatigue and clearance is calculated as follows

Dynamic deflection outside

$$d_{\mathrm{dyn}_{\mathrm{out}}}(x) = \sum_i = 1 \ldots 12\,[d_i(x) w_{i_{\mathrm{out}}}]. \quad (22)$$

Dynamic deflection inside

$$d_{\mathrm{dyn}_{\mathrm{in}}}(x) = \sum_i = 1 \ldots 12\,[d_i(x) w_{i_{\mathrm{in}}}]. \quad (23)$$

Maximum dynamic deflection outside the wheel for determining fatigue and clearance for v = 30, 50, 70, 80 and 90 kmph is

$$d_{\mathrm{dyn}_{\mathrm{out}_{\mathrm{fat}}}} = \mathrm{MAX}[d_{\mathrm{dyn}_{\mathrm{out}}}(x)]. \quad (24)$$

Maximum dynamic deflection inside the wheel for determining fatigue and clearance for v = 30, 50, 70, 80 and 90 kmph is

$$d_{\mathrm{dyn}_{\mathrm{in}_{\mathrm{fat}}}} = \mathrm{MAX}[d_{\mathrm{dyn}_{\mathrm{in}}}(x)]. \quad (25)$$

FST static vertical deflections

Using eqs (15) and (16), the static vertical deflections outside and inside the wheel are calculated as follows

$$\text{Static deflection } d_{\text{static}} = F_{\text{static}} / k_{v_{\text{FST}}}. \quad (26)$$

Static deflection – outside

$$d_{\text{static out}} = F_{\text{static out}} / k_{v_{\text{FST out}}}. \quad (27)$$

Static deflection – inside

$$d_{\text{static in}} = F_{\text{static in}} / k_{v_{\text{FST in}}}. \quad (28)$$

FST dynamic horizontal deflections

To calculate the dynamic horizontal deflections outside and inside the wheel, the horizontal component of traffic load on the track and load distribution between the axles in adjacent bogies should be considered. Using eq. (16), the maximum dynamic horizontal deflection for $v = 30$, 50, 70, 80 and 90 kmph is calculated as

$$d_{\text{dyn HOR fn}} = (F_{\text{centr H}} - F_{\text{vert H}})12 \text{ axles}/ ((x_{\text{axle 12}} - x_{\text{axle 1}})k_{\text{H}_{\text{FST}}}). \quad (29)$$

Using eq. (16) and taking the effect of transverse load outside and inside the wheel, maximum dynamic horizontal deflection is determined for fatigue and clearance as

$$d_{\text{dyn HOR fat}} = F_{\text{res H out}} 12 \text{ axles} / ((x_{\text{axle 12}} - x_{\text{axle 1}})k_{\text{H}_{\text{FST}}}. \quad (30)$$

FST static horizontal deflection

Using eqs (16) and (17), the static horizontal deflections outside and inside the wheel is calculated as

$$d_{\text{static HOR}} = F_{\text{est}} \text{sen}\theta / k_{\text{HLF}}. \quad (31)$$

FST vertical natural frequency

Using eqs (24)–(26) and considering the unsprung train mass, the vertical natural frequency of FST is calculated as

$$f_{n\text{train}} = 5/[(((d_{\text{dyn OUT fn}} + d_{\text{dyn IN fn}})/2)m_{\text{train fn}} + d_{\text{static}})/10]^{1/2}. \quad (32)$$

The calculation of insertion loss based on vertical natural frequency and damping ratio of MSS (spectral analysis in third-octave bands) depends on the transmissibility (T), which is expressed as

$$T = [(1 + 4D^2\eta^2)/((1 - \eta^2)24D^2\eta^2)]^{0.5}, \quad (33)$$

where η is the tuning ratio and D is the damping ratio related to critical damping.

Results and discussion

The static and dynamic responses and natural frequency of steel MSS are calculated based on the influence lines (Zimmermann method). Table 2 lists the design parameters of MSS. In this study for speed ranging from 30 to 90 kmph, the diameter of the tunnel is taken as 5.8 m. This study shows that as the speed of the train increases, the required cant will also increase. Therefore, to design an economical section, the longitudinal spacing and radius of the curve must be adjusted accordingly. Also, fatigue verification of steel MSS must be done and it should be under permissible limits.

Impact of speed on curve radius and cant

The safest design for different values of speed/radius/cant has been made. If the curve radius is 200 m, then it will be difficult to run the train at a speed above 30 kmph. Therefore, a practical design has been suggested in this study with varying train operating speed, curve radius and actual site conditions. In this study, 30–90 kmph speed of the train has been taken with radius varying

Table 2. Steel MSS design parameters

Diameter (m)	5.8
Maximum axle load (kN)	160
Minimum axle load (kN)	85
Rail type	UIC60
Critical damping ratio	8%
Dynamic factor/overload factor	1.49
Width of the floating slab track (FST), b(m)	2.758
Width of the side beams b_1 (m)	0.387
Width of the central beam b_2 (m)	1.000
Width of the side triangles b_3 (m)	0.487
Height of FST without beams h (m)	0.338
Height of the longitudinal beams h_1 (m)	0.122
Centre of Gravity (CoG) of slab, CoG (m)	0.214
Braking load – 12.5% of the vertical axle load (kN)	20
Length of wagon, C_{wag} (m)	25
Height of wagon, h_{wag} (m)	4.048
Width of wagon, b_{wag} (m)	3.20
Number of axles n_{axles}	12
Axle spacing in the same bogie (m)	2.5
Unsprung train mass (part of the train mass oscillating at the same degree of freedom as the track slab)	15%
Vertical spring stiffness k_{v} (kN/mm)	6.63
Horizontal spring stiffness k_{H} (kN/mm)	4.93
Static load – FST weight (kN/m single track)	36.23

Table 3. Design calculations for steel MSS

Speed (kmph)	30	50	70	80	90
Characteristic length of FST (m)	4.33	4.26	4.23	4.23	4.23
Radius (m)	200	280	400	520	660
Cant (mm)	50.79	100.77	138.26	138.92	138.52
Longitudinal spacing (m)	1.55	1.45	1.41	1.405	1.4
Centrifugal force (kN/axle)	5.56	11.02	15.12	15.19	15.15
Resultant vertical load outside wheel (kN)	86.61	93.12	97.99	98.08	98.03
Resultant vertical load inside wheel (kN)	73.39	66.89	62.01	61.92	61.97
Static deflection – inside (mm)	4.23	3.96	3.85	3.84	3.83
Static deflection – outside (mm)	4.23	3.96	3.85	3.84	3.83
Vertical stiffness per metre length of FST (kN/mm)	8.55	8.70	9.40	8.97	9.00
Horizontal stiffness per metre length of FST (kN/mm)	6.36	6.65	6.99	6.86	6.88

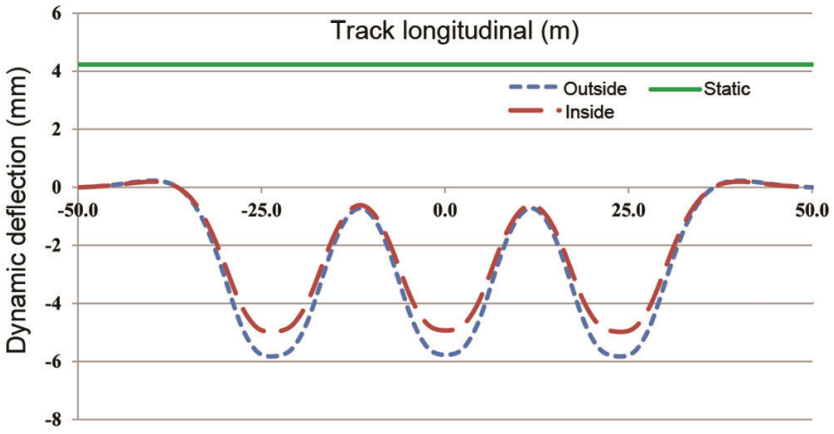

Figure 3. Vertical static and dynamic deflections of MSS at 30 kmph speed.

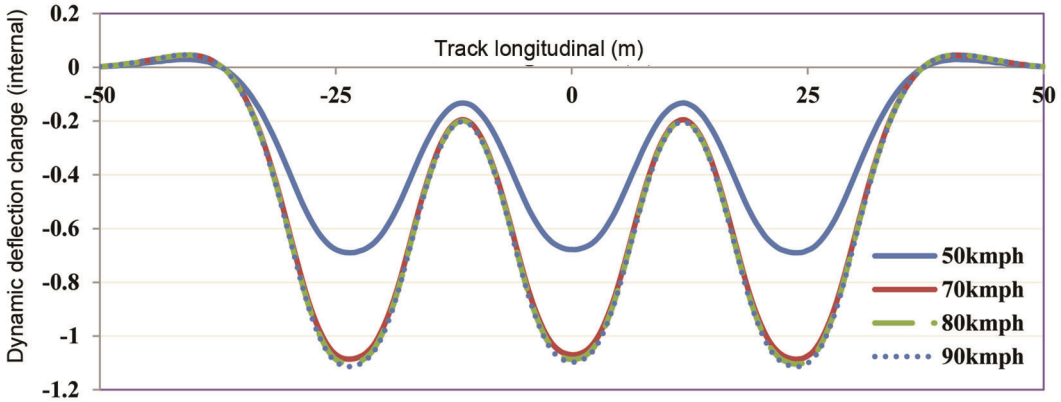

Figure 4. Change in dynamic deflection in the inside track with respect to 30 kmph speed.

from 200 to 660 m (Table 3). It is observed that as the speed of the train and curve radius increase, the cant will also increase. It is 50.79 mm at 30 kmph and 138.52 mm at 90 kmph, which is found to be under permissible limits. The most critical section begins where the radius of the tunnel is less than 350 m. At this radius, vibration attenuation becomes a major problem due to interaction between rail and wheel. Here, speed plays a minor role.

Static and dynamic responses of MSS

Vertical static and dynamic deflections play an important role while designing MSS. There are two types of dynamic deflection, namely dynamic deflection of the outside and inside tracks (Figures 3–5). As the speed of the train increases from 30 to 90 kmph, the maximum dynamic deflection outside the track decreases from 5.83 to

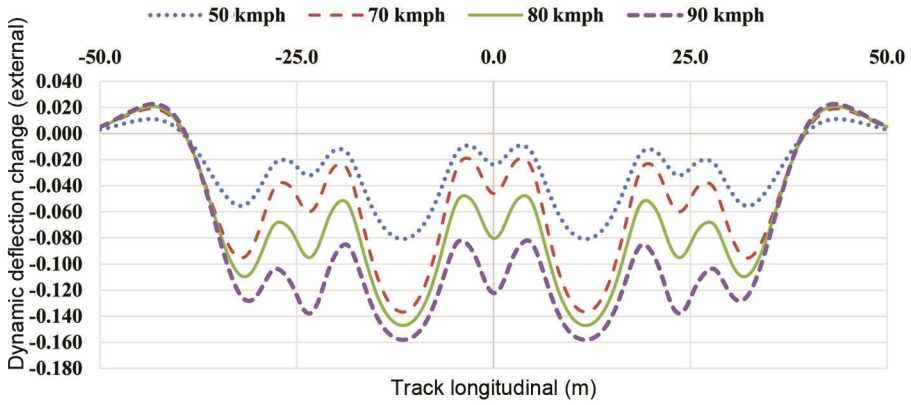

Figure 5. Change in dynamic deflection in the outside track with respect to 30 kmph speed.

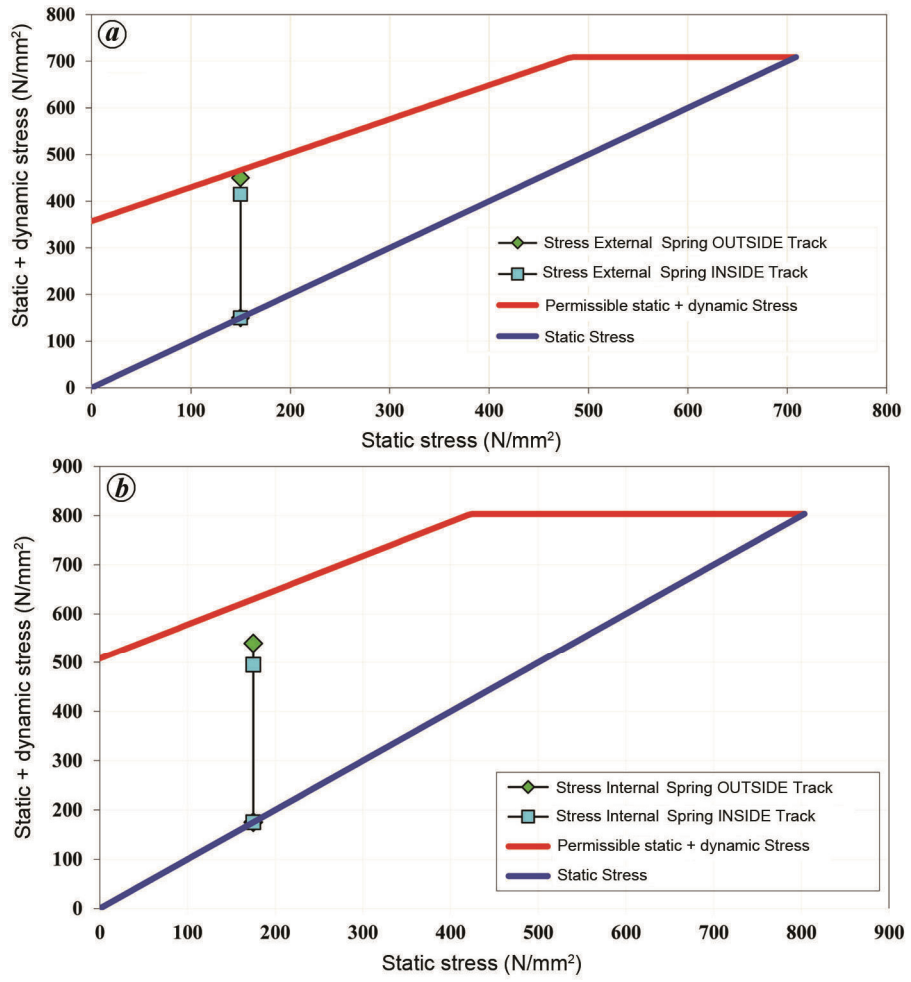

Figure 6. ***a***, Stresses in the external springs on the outside and inside tracks at 30 kmph speed. ***b***, Stresses in the internal springs on the outside and inside tracks at 30 kmph speed.

5.69 mm. The maximum dynamic deflection for the inside track starts decreasing with increase in speed, i.e. 4.98 to 3.87 mm. The reason for this declining trend is that with the increase in train speed, the static effect of the load decreases. It is observed that the static deflection of the outside track and the inside track follows decreasing trend, i.e. 4.23 mm at 30 kmph and 3.83 mm at 90 kmph (Table 3). Steel MSS used in this study has been designed for 9.71 mm, which is the permissible dynamic deflection amplitude. It is observed that the maximum deflection for

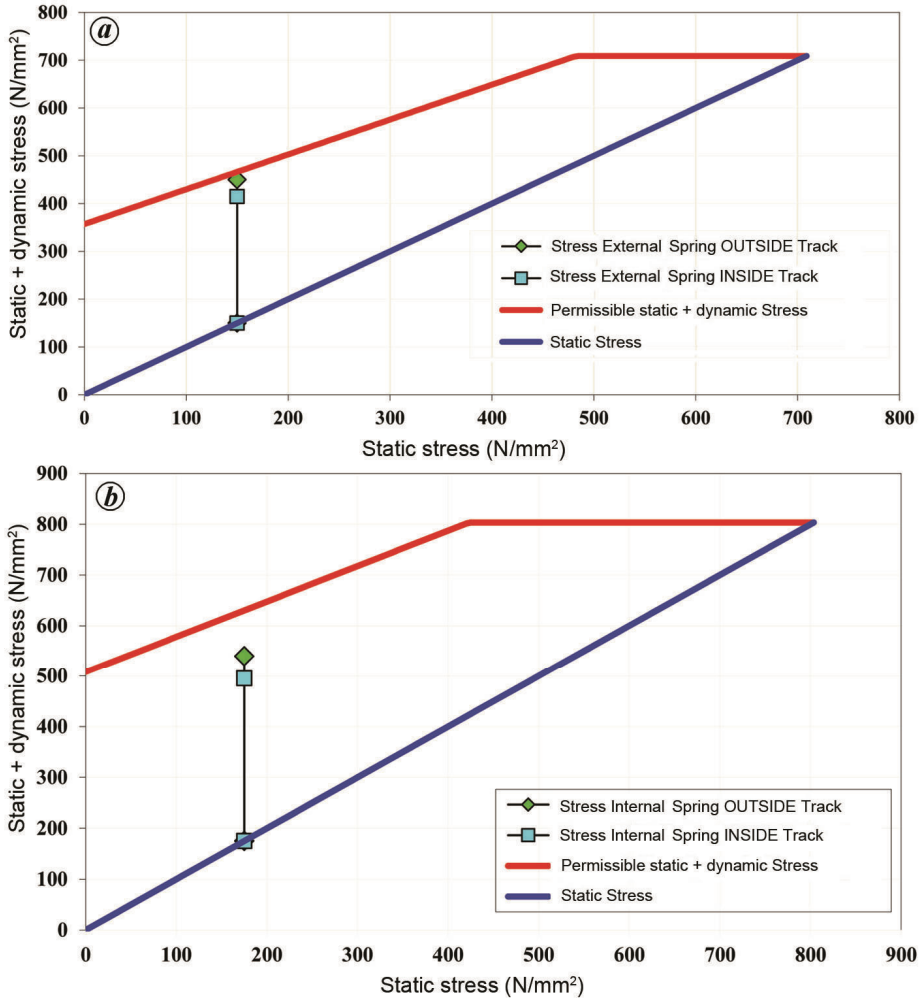

Figure 7. ***a***, Stresses in the external springs on the outside and inside track. ***b***, Stresses in the internal springs on the outside and inside tracks.

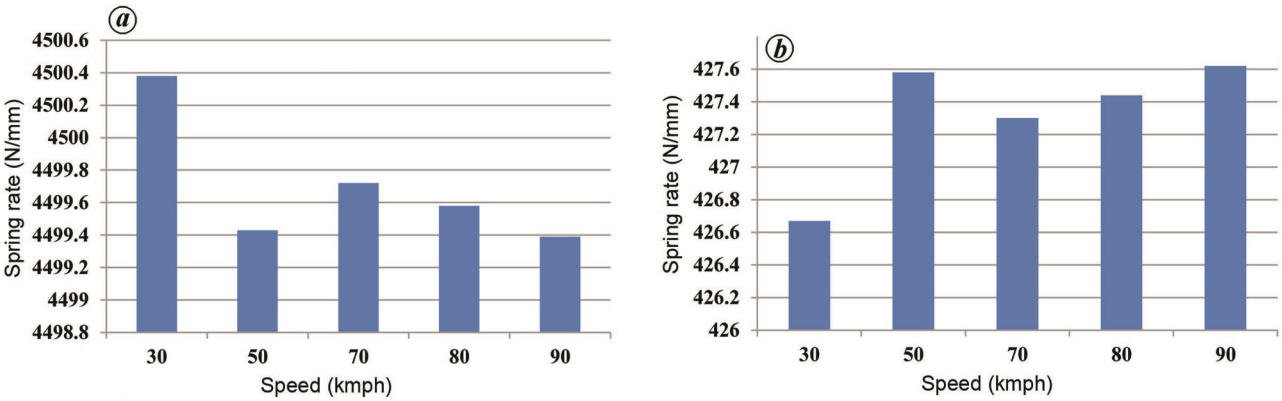

Figure 8. Static and dynamic horizontal spring rate: (***a***) external and (***b***) internal.

the design proposed in this study is under permissible limits, being 5.83 mm on the outside track and 4.98 mm inside the track.

For fatigue verification, the static and dynamic stresses in the internal and external springs must also be under permissible limits according to Goodman Diagram DIN EN 13906-1-2013-11 (Figures 6 and 7). For internal spring, at 0 N/mm^2 the permissible static and dynamic stress is found to be 508 and at 425 N/mm^2; it is 804 N/mm^2 but after 425 N/mm^2 it is linear. Similarly for the external

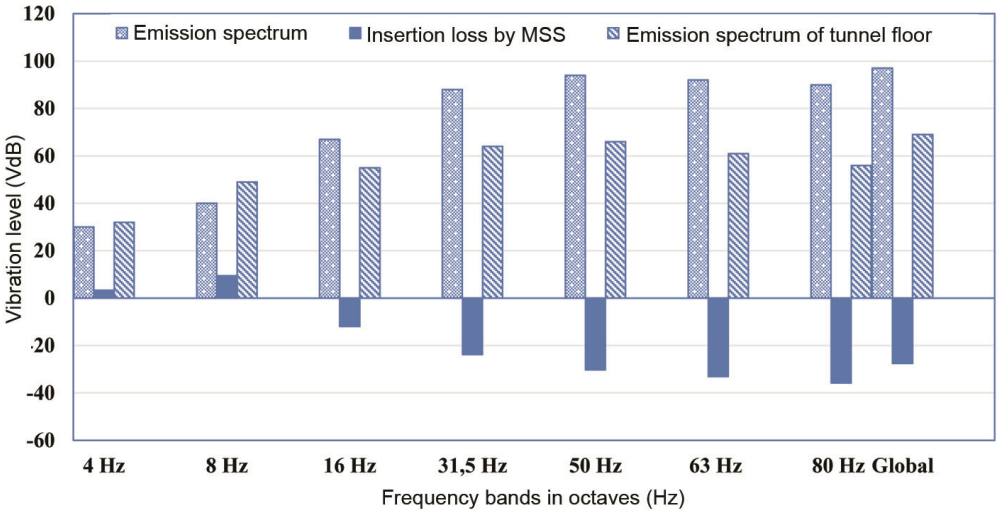

Figure 9. Vibration levels with and without MSS at 30 kmph speed.

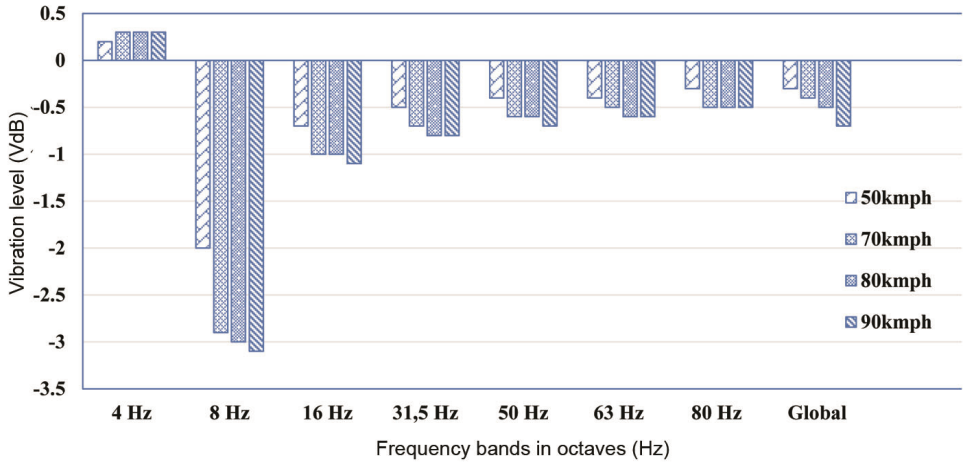

Figure 10. Vibration levels with and without MSS with respect to 30 kmph speed.

spring, at 0 N/mm^2 the permissible static and dynamic stress is found to be 357 N/mm^2 and at 485 N/mm^2 it is 709 N/mm^2; but after 485 N/mm^2 it is linear.

The vertical spring rate in the external and internal springs is constant at each speed. The horizontal spring rate for the external spring is 4500.38 N/mm at 30 kmph and reaches up to 4499.39 N/mm at 90 kmph (Figure 8 *a*). While the horizontal spring rate for the internal spring is 426.67 N/mm at 30 kmph and decreases with increase in speed, i.e. at 90 kmph it is 427.62 N/mm (Figure 8 *b*).

Vertical natural frequency of MSS

The natural frequency of steel MSS is observed to vary between 7.04 and 7.40 Hz (Table 3). It shows that the attenuation should start after 9.95 and 10.46 Hz and go up to 26–28 VdB. This is found to be a good amount of vibration attenuation at source for steel MSS according to RDSO. Figures 9 and 10 show the vibration attenuation with and without application of steel MSS for varying speeds respectively. The vibration level in the tunnel, before application of steel MSS was 90 VdB at 80 Hz, which is well above the permissible limits of 72 VdB (RDSO). However, after application of steel MSS, vibration attenuation was observed. At 80 Hz, there was maximum vibration attenuation of 35.8 VdB at each speed, which is much more than the global attenuation value of 27.5 VdB at 30 kmph, 27.2 VdB at 50 kmph, 27.1 VdB at 70 kmph, 27 VdB at 80 kmph and 26.8 VdB at 90 kmph. The emission from the tunnel floor remains constant at each speed; it is 32 VdB at 4 Hz and 56 VdB at 80 Hz.

Table 3 shows that when the train speed increases from 30 to 90 kmph, the characteristic length of FST and the longitudinal spacing between the MSS show a decreasing trend. The resulting load for calculating the natural

frequency and for verifying the tunnel clearance and fatigue of the outside wheel, increases with train speed. It is 86.61 kN at 30 kmph and 98.03 kN at 90 kmph. The resulting vertical load for the inside wheel decreases with increasing speed; it is 73.39 kN at 30 kmph and 61.97 kN at 90 kmph. It is also observed that the vertical stiffness per metre length of FST of the single trackbed is 8.55 kN/mm at 30 kmph and 9 KN/mm at 90 kmph, while the horizontal stiffness per metre length of FST of the single trackbed is 6.36 kN/mm at 30 kmph and 6.88 kN/mm at 90 kmph. As the natural frequency depends on the stiffness of MSS, it should always be less for higher vibration attenuation.

Conclusion

In this study, the static and dynamic analysis of steel MSS is performed using the Zimmermann method, and the effect of speed, radius and cant on steel MSS has been observed. The following conclusions are drawn from this study.

- As the speed of the train increases, the dynamic deflection both outside and inside the wheel decreases. The maximum dynamic deflection of 5.83 mm is found to be under the permissible limits. It has a major effect on the design of MSS.
- As the speed of the train increases, so does the curve radius, which ultimately decreases the characteristic length of FST and thus changes the longitudinal spacing between the MSS, thereby lowering the cost and making the design economical.
- For a cost-effective design, in the curve section, steel MSS should be provided for a length of 150 m on both sides from the centre of the curve, while on the straight section, discrete PU MSS must be used.
- The insertion loss (vibration attenuation) depends on the natural frequency of steel MSS; lower the natural frequency, greater will be the insertion loss, and vice-versa. As the speed of the train increases, the stiffness of MSS also increases, leading to an increase in the natural frequency of MSS, which directly affects the vibration attenuation of steel MSS.
- All results have been verified with the fatigue test and correspond to the Goodman diagram.

Conflict of interest: The authors declare no conflict of interests.

1. Jones, C. J. C. and Block, J. R., Prediction of ground vibration from freight trains. *J. Sound Vib.*, 1996, **193**(1), 205–213.
2. Gordon, C. G., Generic vibration criteria for vibration-sensitive equipment. *Proc. SPIE*, 1999, 22–39.
3. ISO-2631-1:1997(E) Part-1, Mechanical vibration and shock – evaluation of human exposure to whole-body vibration – Part 1: general requirements, 1997.
4. Volberg, G., Propagation of ground vibrations near railway tracks. *J. Sound Vib.*, 1983, **87**(2), 371–376.
5. Bata, M., Effects on buildings of vibrations caused by traffic. *Build. Sci.*, 1985, **99**(1), 1–12.
6. Wilson, G. P., Saurenman, H. J. and Nelson, J. T., Control of ground-borne noise and vibration. *J. Sound Vib.*, 1983, **87**(2), 339–350.
7. Xue, Y., Li, S., Zhang, D., Sun, X., Sun, Z. and Nie, Y., Vibration characteristics and environmental responses of different vehicle–track–ballast coupling systems in subway operation. *J. Vibroeng.*, 2014, **16**(5), 2458–2473.
8. Woods, R. D., Screening of surface waves in soils. *J. Soil Mech. Found. Div. ASCE*, 1968, **94**, 951–979.
9. Talbot, J. P. and Hunt, H. E. M., On the performance of base-isolated buildings. *Build. Acoust.*, 2000, **7**(3), 163–178.
10. Cox, S. J., Wang, A., Morison, C., Carels, P., Kelly, R. and Bewes, O. G., A test rig to investigate slab track structures for controlling ground vibration. *J. Sound Vib.*, 2006, **293**(3–5), 901–909.
11. Zhou, M., Wei, K., Zhou, S., Xiao, J. and Gong, Q., Influence of different track types on the vibration response of the jointly-built structure of subway and the buildings. *China Railw. Sci.*, 2011, **32**(2), 33–40.
12. Yan, Z. Q., Markine, V., Gu, A. J. and Liang, Q. H., Optimization of the dynamic properties of ladder track to control rail vibration using the multipoint approximation method. *J. Vib. Control*, 2014, **20**(13), 1967–1984.
13. Raju, R. K. and Vineeth, V. D., Developments in vibration control of structures and structural components with magnetorheological fluids. *Curr. Sci.*, 2017, **112**(3), 499–508.
14. Lopes, P., Costa, P. A., Calcada, R. and Cardoso, A. S., Mitigation of vibrations induced by railway traffic in tunnels through floating slab systems: numerical study. In Eurodyn 2014: 9th International Conference on Structural Dynamics, Proto, Portugal, 2014, pp. 871–878.
15. Grootenhuis, P., Floating track slab isolation for railways. *J. Sound Vib.*, 1977, **51**(3), 443–448.
16. Nelson, J. T., Recent developments in ground-borne noise and vibration control. *J. Sound Vib.*, 1996, **193**(1), 367–376.
17. Kurzweil, L. G., Ground-borne noise and vibration from underground rail systems. *J. Sound Vib.*, 1979, **66**, (3), 363–370.
18. Hussein, F. M. and Hunt, E., Modelling of floating-slab track with discontinuous slab. Part 1: response to oscillating moving loads. *J. Low Frequen. Noise Vib. Active Control*, 2006, **25**(1), 23–39.
19. Lombaert, G., Degrande, G., Vanhauwere, B., Vandeboght, B. and Francois, S., The control of ground-borne vibrations from railway traffic by means of continuous floating slabs. *J. Sound Vib.*, 2006, **297**(3–5), 946–996.
20. Hussein, M. F. M. and Hunt, H. E. M., Modelling of floating-slab tracks with continuous slabs under oscillating moving loads. *J. Sound Vib.*, 2006, **297**(1–2), 37–54.
21. Kuo, C., Huang, C. and Chen, Y., Vibration characteristics of floating slab track. *J. Sound Vib.*, 2008, **317**(3–5), 1017–1034.
22. Zhou, B., Xie, X. Y. and Yang, Y. B., Simulation of wave propagation of floating slab track–tunnel–soil system by 2D theoretical model. *Int. J. Struct. Stabil. Dyn.*, 2014, **14**, 1–24.
23. Connolly, D. P., Kouroussis, G., Laghrouche, O., Ho, C. L. and Forde, M. C., Benchmarking railway vibrations – track, vehicle, ground and building effects. *Constr. Build. Mater.*, 2015, **92**, 64–81.
24. Lei, X. Y. and Jiang, C. D., Analysis of vibration reduction effect of steel spring floating slab track with finite elements. *J. Vib. Control*, 2016, **22**, 1462–1471.
25. Ding, D. Y., Liu, W. N., Li, K. F., Sun, X. J. and Liu, W. F., Low frequency vibration tests on a floating slab track in an underground laboratory. *J. Zhejiang Univ.-Sci. A*, 2011, **12**, 345–359.
26. Zhu, S., Wang, J., Cai, C., Wang, K. and Zhai, W., Development of a vibration attenuation track at low frequencies for urban

rail transit. *Comput-Aided Civ. Infrastruct. Eng.*, 2017, **32**, 713–726.
27. Hussein, M. F. M., A comparison between the performance of floating slab tracks with continuous and discontinuous slabs in reducing vibration from underground railway tunnels. In 16th International Congress on Sound and Vibration Karakow, Poland, 2009, pp. 46–51.
28. Liu, W., Ding, D., Li, K. and Zhang, H., Experimental study of the low-frequency vibration characteristics of steel spring floating slab track. *Tumu Gongcheng Xuebao/China Civ. Eng. J.*, 2011, **44**, 118–125.
29. Li, K., Liu, W., Sun, X., Ding, D. and Yuan, Y., In-site test of vibration attenuation of underground line of Beijing metro line 5. *J. China Rail. Soc.*, 2011, **33**, 112–118.
30. Cui, F. and Chew, C. H., The effectiveness of floating slab track system – Part I. Receptance methods. *Appl. Acoust*., 2000, **61**, 441–453.
31. Chandra, S. and Agarwal, M. M., *Railway Engineering*, Oxford University Press, New Delhi, 2007.
32. DIN EN 13906-1, Cylindrical helical springs made from round wire and bar – calculation and design – Part-1: compression springs, 2013–11, pp. 1–39.
33. IS 456: Plain and Reinforced Concrete – Code of Practice, 2000.
34. Bombardier Movia Metro for New Delhi.
35. BS EN 13674-1, Railway applications – track–rail – Part 1: vignole railway rails 46 kg/m and above (includes Amendment A1), 2017.
36. Research Design and Standards Organization (RDSO)-ISO-9001, Ministry of Railways, Government of India, 2015.
37. Federal Transit Administration, Transit Noise and Vibration Impact Assessment Manual. FTA Report No. 0123, National Transportation Systems Center, US Department of Transportation, 2018, pp. 1–243.

ACKNOWLEDGEMENTS. We thank the Academy of Scientific and Innovative Research–Central Road Research Institute, New Delhi, and the Transport Planning and Environment Division, CSIR-Central Road Research Institute, New Delhi for their help and collaboration during this study.

Received 12 January 2021; revised accepted 20 September 2021

doi: 10.18520/cs/v121/i11/1441-1451